

# Spring and summer potential flood risk in Northeast China

Wei Qi<sup>a</sup>, Lian Feng<sup>a,\*</sup>, Hong Yang<sup>b,c</sup>, Junguo Liu<sup>a</sup>

<sup>a</sup> School of Environmental Science and Engineering, Southern University of Science and Technology, Shenzhen 518055, China

<sup>b</sup> Eawag, Swiss Federal Institute of Aquatic Science and Technology, Dübendorf, Switzerland

<sup>c</sup> Department of Environmental Science, MGU, University of Basel, Basel, Switzerland

## ARTICLE INFO

### Keywords:

Snow  
Flood  
Northeast China  
GDP  
Crop production  
Hydrological risk

## ABSTRACT

*Study region:* Northeast China

*Study focus:* Northeast China is an important region for industry and agriculture in China. In this region, investigations are lacking on the spatial distribution of snow melt contributions to the spring maximum runoff/discharge, and no studies have compared the spring and summer potential flood risks. Here, for the first time in Northeast China, we investigated the spatial distribution of snow melt contributions to spring maximum runoff/discharge and compared the spring and summer potential flood risks in terms of their spatial distributions, crop production and economic exposures.

*New hydrological insights for the region:* We find that snow contributes approximately three-fourths of spring maximum floods from 1982 to 2011. On average, potential economic exposures to the summer and spring floods represent 3.9% and 0.4% of total GDP, respectively. Potentially exposed production of maize, rice and soybean to summer floods accounts for approximately 2.8% of the total, and potentially exposed wheat production to the spring floods accounts for 0.3% of the total. GDP growth amplifies increasing trends of potential economic exposure, while changes in potential crop production exposure are dominated by flood variations. This study is unique in that snow melt contributions to the spring maximum floods are quantified and that potential GDP and crop production exposure risks to spring and summer floods are quantified and compared for the first time in Northeast China.

## 1. Introduction

There are two types of floods in regions with a cold winter and rainy summer. Because of the cold, precipitation in the winter has the potential to fall as snow with the snow melting in the spring, causing spring floods; in the summer, these regions suffer from heavy rainfall which also results in flooding floods. Northeast China is a region with both spring floods and heavy summer rainfall induced floods (Yang et al., 2020). Because Northeast China is an important region for industry and has a large area of cropland (Yang et al., 2007; Kent et al., 2017; Xin et al., 2020), floods could cause damage to both economic growth and crop production (Zhang et al., 2015, 2016; Chen et al., 2018, 2019; Fu et al., 2018).

Investigations into the spatial distribution of snow melt contributions to spring maximum runoff/discharge and comparisons between spring flood disasters and summer heavy rainfall flood disasters are key issues in extreme flood studies in Northeast China. Currently, studies on the spring snow melt, spring floods and comparisons between spring floods and summer floods remain limited in

\* Corresponding author.

E-mail addresses: [qiw@sustech.edu.cn](mailto:qiw@sustech.edu.cn) (W. Qi), [fengl@sustech.edu.cn](mailto:fengl@sustech.edu.cn) (L. Feng).



the region. For example, Tian et al. (2018) studied spring snow melt runoff in the Second Songhua River (accounting for only 1.5% of the area of Northeast China) based on an empirical approach; Yang et al. (2020) studied flood generation mechanisms in Northeast China with regards to snow melt influence. Although previous studies have investigated the snow influence on floods, the quantitative analysis of snow melt contribution to the spring maximum runoff/discharge is limited, let alone the spatial distribution of the spring flood risk.

In flood risk studies, potential flood risk corresponds to the worst scenario in which there is no flood mitigation infrastructure. Flood risk management aims to reduce and/or avoid potential flood risk. The spatial distribution of potential flood risk can provide information on the locations that are vulnerable to floods, and therefore, region-specific measures can be deployed to reduce flood risk. Therefore, knowing the potential flood risk is the first step for making strategic flood adaptation measures and evaluating the benefits of deploying flood risk management measures. However, the spring and summer potential flood risk studies have not been conducted on the entire Northeast China.

Here, for the first time in Northeast China, we investigated the spatial distribution of snow melt contributions to the spring maximum runoff/discharge and compared spring and summer potential flood risks in terms of their spatial distributions, crop production and economic (i.e., Gross Domestic Product, GDP) exposures. This study is unique in which the snow melt contribution to spring maximum floods is quantified and that the potential crop production and economic exposures to the spring and summer floods are determined and compared.

## 2. Study region, datasets and methodology

The study region covers an area of 1.2 million km<sup>2</sup> (Fig. 1). The Water and Energy Budget-based hydrological model with biosphere and improved snow physics (WEB-DHM-S) was used after calibration and validation against discharge in the study by Qi et al. (2020). WEB-DHM-S combined the hydrological model based on geomorphology developed by Yang (1998), the Simple Biosphere scheme (SIB2) land surface model, and a physically based snowmelt module (Wang et al., 2009a, 2009b, 2009c, 2017; Shrestha et al., 2010). This model has been implemented in numerous studies and has shown good performance (Qi et al., 2015, 2016, 2018, 2019; Wang et al., 2017). More details about the study region, model calibration, model validation, input data and model parameters used can be found in the study by Qi et al. (2020). The simulated runoff by WEB-DHM-S was used as the input of a 2-dimensional hydraulic model (i.e., CaMa-Flood) to simulate the water level, flood inundation area and inundation area fraction distribution (Yamazaki et al., 2011, 2013). Methodology regarding economic and crop production exposures to floods and attribution of the exposures to GDP/crop production variations and climate variations can be found in the Supporting Information. The gridded GDP datasets are available from 1990 to 2015 (Kummu et al., 2018), which have a spatial resolution of 0.08 degrees. Crop yield data of maize, rice, soybean and spring wheat are from the study by Iizumi and Sakai (2020), and the yield data from 1982 to 2011 are used in this study, with a spatial resolution of 0.5 degrees. The yield is from census statistics of the United Nations and was compiled and published by Iizumi and Sakai (2020). We regridded the GDP dataset and crop yield data into 0.1 degree cells to match the grids in the flood simulation using the WEB-DHM-S and CaMa-Flood models. In our study region, spring refers to March, April and May. Summer starts in June and ends in the middle of September, and the annual maximum floods occur in the summer. The main growing season for wheat is the spring, and exposure to spring floods is calculated only for wheat. Because reservoirs and dikes were not considered, the flood risk and exposures represent potential values in this study.

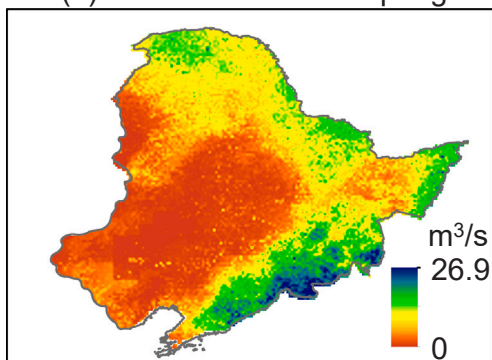
## 3. Results and discussion

### 3.1. Model evaluation

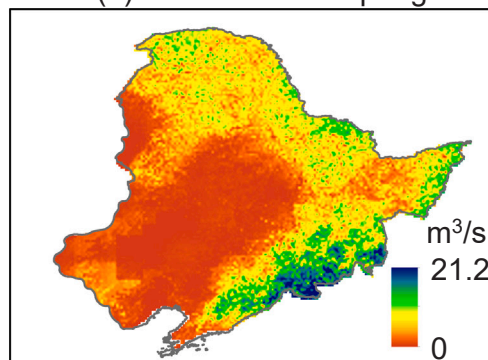
In the discharge simulation, the Nash-Sutcliffe efficiency coefficient and relative bias are 0.81 and 7.8%, respectively (Qi et al., 2020), indicating that the model performance is acceptable. The simulation can reasonably replicate the spatial distribution of satellite-observed water bodies (Fig. S1). There are many saline lakes in the study regions (Zhu et al., 2020). Because saline lakes are not connected with rivers, model simulations cannot simulate their spatial distribution. However, this does not influence potential flood risk analysis due to saline lakes being unable to store spilled river water during flooding. Satellite observations include reservoir and dike influences. The reservoir distribution developed by Lehner et al. (2011) and Messenger et al. (2016) could not include all reservoirs, especially those built in recent years, which could contribute to the differences between model simulations and satellite observations. In the Liao River, the maximum flood depth is less than 3 m (shown in Section 3.3), and flood dikes are usually approximately 1.5 m or 2.0 m. The satellite-observed flood inundation area is after the flood dike functions and therefore shows a smaller water body area than the model simulation.

The simulation can reasonably replicate the seasonal variations in water levels (Fig. S2), with R being at least 0.68. In addition, the simulation can imitate the average water level well with  $|RB| \leq 0.3\%$ . The uncertainty in water level simulation may result from river bathymetry uncertainty, such as river depth and width. River depth is derived based on empirical power-law approaches in the CaMa-Flood model because there is no observation; river width is based on empirical power-law estimation combined with satellite observations since satellite observation availability is limited in regions (Yamazaki et al., 2012, 2013). The input data, especially precipitation, could influence the simulation. However, we have used the best publicly available precipitation in the region (Qi et al., 2016). In addition, human activities could change natural river bathymetry. For example, river channels were destroyed in some regions after the 1998 mega-flood and then restored by human activities. Furthermore, there are over one hundred reservoirs in Northeast China, and the model simulation does not consider reservoir operations, which may also cause the differences. Because the

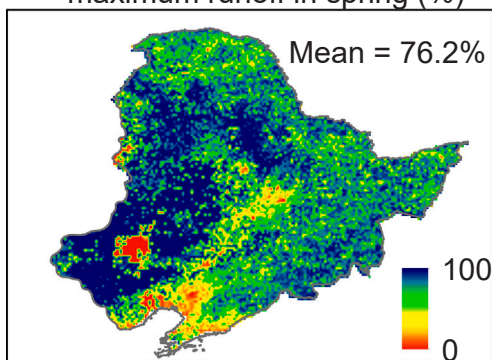
(a) Maximum runoff in spring



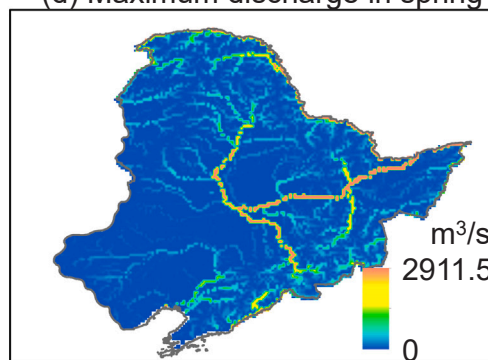
(b) Snow runoff in spring



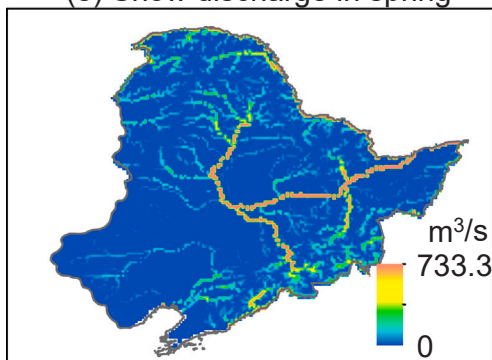
(c) Contribution of snow runoff to maximum runoff in spring (%)



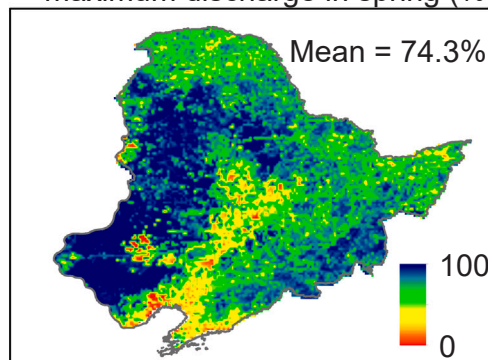
(d) Maximum discharge in spring



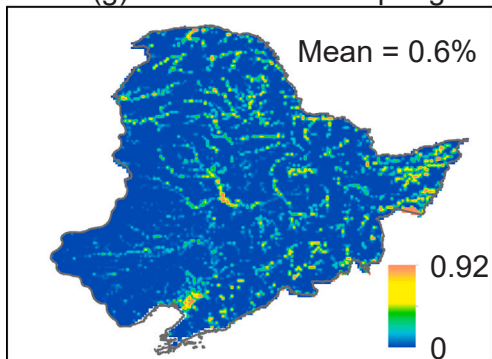
(e) Snow discharge in spring



(f) Contribution of snow discharge to maximum discharge in spring (%)



(g) Flood fraction in spring



(h) Flood depth in spring (m)

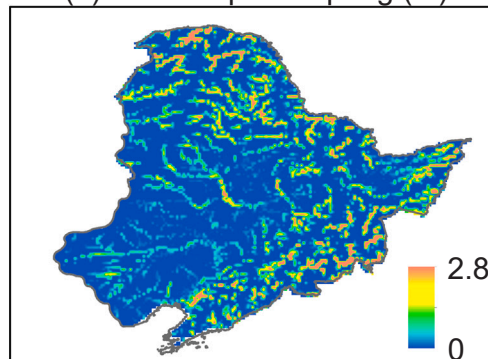


**Fig. 2.** Spring floods. (a) Maximum runoff in spring. (b) Snow runoff corresponding to the maximum runoff. (c) Contribution of snow runoff to maximum runoff. (d) Maximum discharge in spring. (e) Snow discharge corresponding to the maximum discharge. (f) Contribution of snow discharge to maximum discharge. (g) Maximum potential flood area fraction (flood area/total area). (h) Maximum potential flood depth. The results are based on the average data from 1982 to 2011.

Liao River is one of the rivers with the strongest human activity influence in China and discharge in this river is largely influenced by human activities (Liu et al., 2018), we did not choose water level gauges in the Liao River to validate the model simulation.

After evaluations with satellite-observed water body distribution, in situ gauge-observed water levels and discharge, we considered that the model can reasonably simulate flood changes and their influences. Therefore, the model framework will be used in the following sections to study floods, potential crop production and economic exposures to floods.

### 3.2. Spring floods

The southeast regions have a higher intensity of maximum runoff than the other regions, and the middle and southwest regions have lower intensities (see Fig. 2a). Similarly, runoff from snow melt has higher intensity in southeast regions and lower intensity in the middle and southwest regions (Fig. 2b). The contribution of the snow runoff to maximum runoff is higher in the western regions than in the southern regions (Fig. 2c). The regional average contribution of snow melt runoff to maximum runoff is 76.2%. Northern and eastern regions have higher discharge than other regions (Fig. 2d), and the snow discharge in the southern region is smaller (Fig. 2e). The snow discharge contribution to maximum discharge is higher in the western regions and smaller in the southern regions, which are similar to the results of snow runoff contribution to maximum runoff (Fig. 2c). The regional average contribution of snow melt discharge to maximum discharge is 74.3%. The regional average potential flood area fraction of maximum discharge is 0.6% (Fig. 2g), and the potential flood depth in the northern, eastern and southeast regions is higher than that in the southwestern regions (Fig. 2h). Overall, snow melt contributes approximately three-fourths of the spring maximum runoff and discharge, and the contribution of snow melt to discharge is higher in the northern and eastern regions than in the southern regions.

### 3.3. Summer floods

The southern and eastern regions have higher intensity maximum runoff than the western and northern regions (see Fig. 3a), which is different from the spatial distribution of the maximum spring flood. The maximum discharge in the Songhua River is higher than that in the Liao River, which is similar to the maximum discharge in the spring. The middle reach of the Songhua River (Region A) and the lower reach of the Liao River (Region B) are two concentrated regions with large potential flood areas. In Region A, the two largest tributaries of the Songhua River meet in the plain area, i.e., the Neijiang River and the Second Songhua River, and therefore cause a large area to be potentially flooded. In Region B, the main reach of the Liao River meets the Hun River and Taizi River, and they cause the large potential flooding area together.

### 3.4. Temporal changes of the summer and spring floods

The summer maximum potential flood area is decreasing (Fig. 4a). The decreasing trend resulted from the reduced annual maximum precipitation (Fig. 4c). The average annual maximum potential flood area is 33,000 km<sup>2</sup>. The results also show that the spring maximum potential flood area is increasing (Fig. 4b), which is different from the changes in the annual maximum potential flood area. The increasing trends may result from the increasing maximum precipitation in the spring (Fig. 4e). However, the snow runoff ratio is significantly decreasing (Fig. 4d), implying that the potential spring flood risk resulting from snow melt is decreasing. The average spring potential flood area is 5000 km<sup>2</sup>. Overall, the annual maximum potential flood risk is decreasing, and the spring potential flood risk is increasing, but the contribution from snow melt is decreasing.

### 3.5. Crop production exposure to floods

The potential exposure to summer floods for maize crops is decreasing in the situations of considering and without considering the increasing maize production (Fig. 5a and Fig. S4a). Fig. 5b clearly shows that flood variations dominate the potential maize production exposure to summer floods, and the maximum contribution from maize production increase was 39% in 2011. Similarly, potential rice and soybean production exposure to summer floods decreased as well, although the total production of rice and soybean increased (Fig. S4b and c). These decreases are also due to summer flood variations (Fig. 5d and f). In contrast to maize, rice and soybean, the potential exposure of wheat to spring floods is increasing, although total spring wheat production in Northeast China is decreasing (Fig. S4d), which is due to the intensification of spring floods (Fig. 4b). Fig. 5h also clearly shows that potential spring wheat production exposure to spring floods is dominated by flood variations in most years. The multiyear mean potentially exposed production of maize, rice and soybean to summer floods are 2.8%, 2.9% and 2.8% (equivalent to  $4.6 \times 10^6$  t,  $5.7 \times 10^6$  t and  $1.4 \times 10^6$  t, respectively), and potential spring wheat production exposure to spring floods is 0.3% (equivalent to  $4.5 \times 10^5$  t).

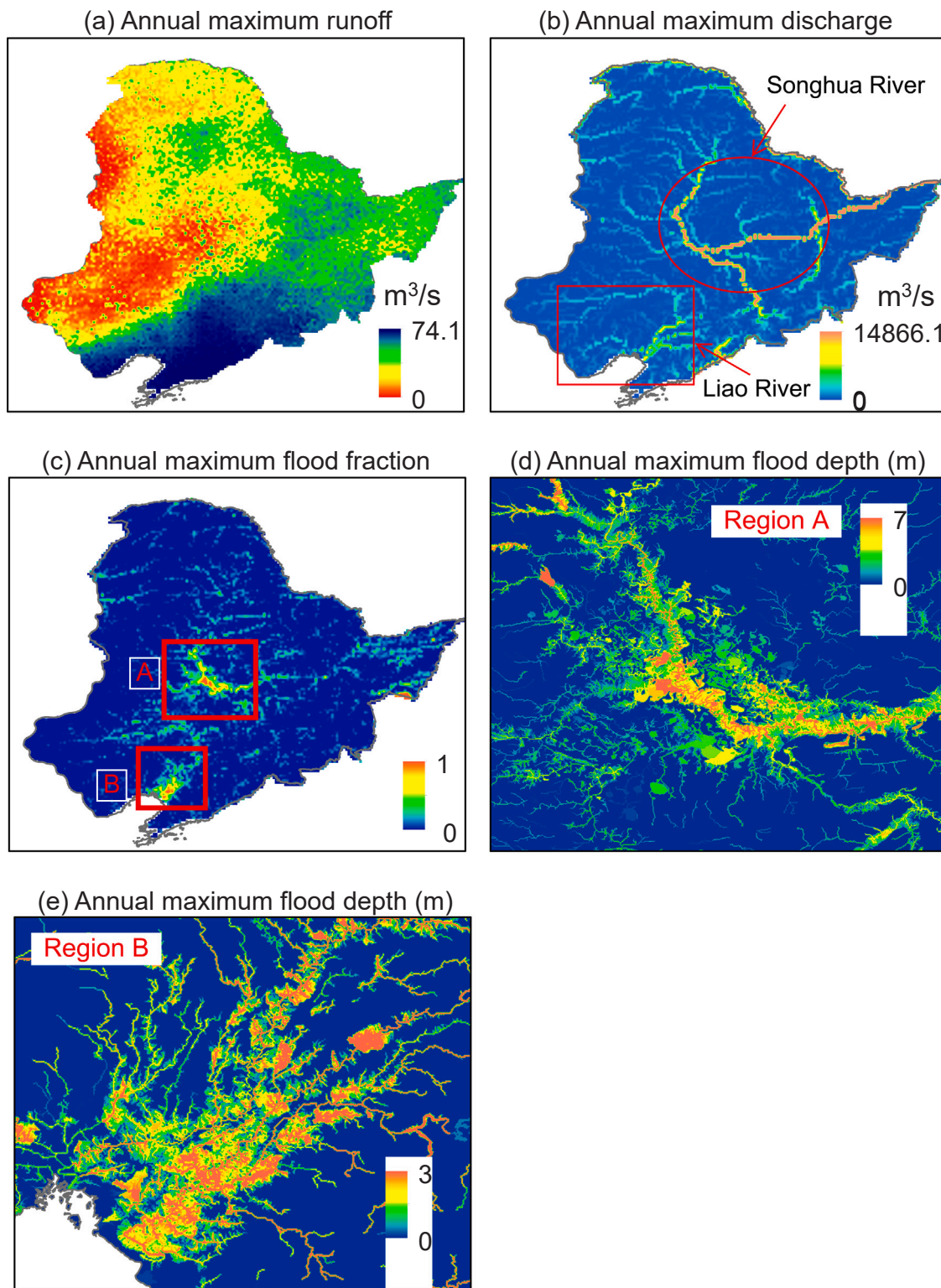


Fig. 3. Summer floods. (a) Mean maximum runoff. (b) Mean maximum discharge. (c) Mean maximum potential flood fraction. (d) and (e) Mean maximum potential flood depth with 500 m spatial resolution. The results are based on the average data from 1982 to 2011.

3.6. Economic exposure to floods

Fig. 6 shows the potential economic exposure to summer maximum floods and spring maximum floods and the attribution of the potential exposure to GDP growth and flood variations. The potential exposure decreases when only considering climate variations, which is the same as the trend of summer maximum potential flood area (Fig. 4a). However, the overall potential exposure considering both climate variation and enlargement of economic volume is increasing, which is different from the trends of the summer maximum potential flood area, implying that enlargement of economic volume plays a primary role in the increases of the potential economic exposure. The results in Fig. 6b underpin the contribution of the enlargement of economic volume to the rapidly increasing potential exposure, indicating that economic development exacerbates potential economic exposure. Fig. 6c also shows that potential economic exposure to spring floods is increasing when considering both climate variation and GDP growth. Different from the potential exposure to summer maximum flood, the potential exposure to the spring flood is increasing when only considering flood variations, which is due to the increasing spring maximum runoff, as shown in Fig. 4d. However, the slope of the trend in considering both flood variation and GDP growth is much greater than that of only considering flood variations. This result indicates that GDP growth plays an important role in the increases in potential economic exposure, which is also confirmed by the results in Fig. 6d. The potential economic exposure to spring floods accounts for 0.4% (equivalent to  $\$1.8 \times 10^9$ ) of the total GDP of Northeast China on average from 1990 to 2011, and it is 3.9% (equivalent to  $\$1.4 \times 10^{10}$ ) for summer floods. Overall, enlargement of economic volume exacerbates the increasing trends of potential economic exposure to both the summer maximum floods and spring maximum floods, potential exposure

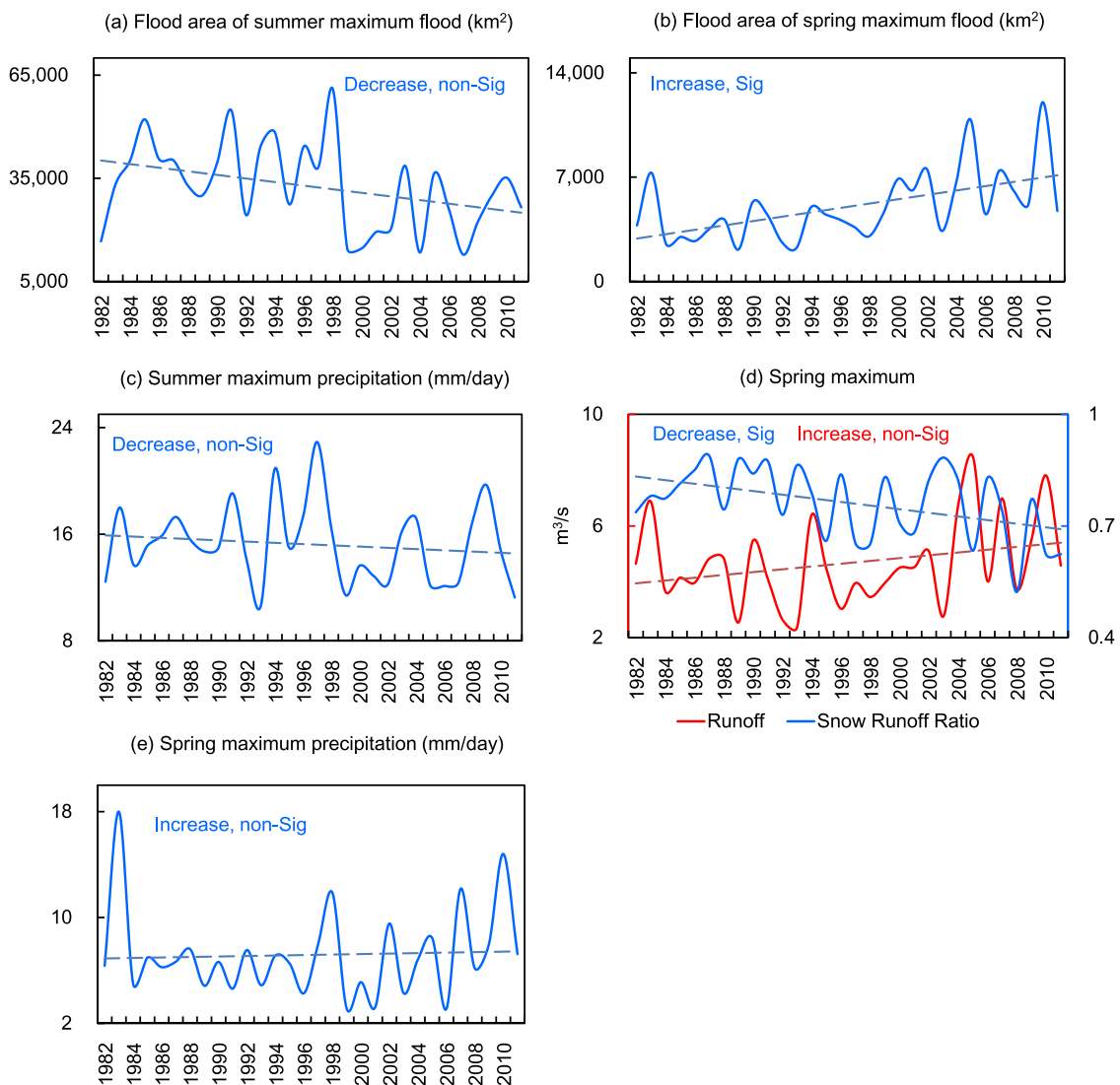
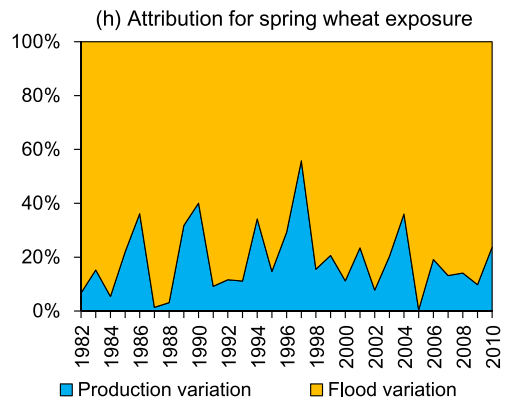
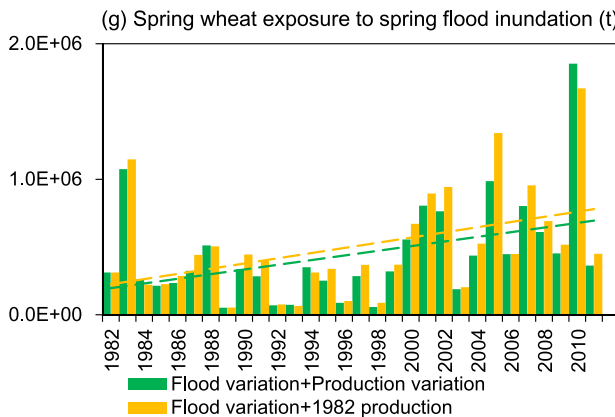
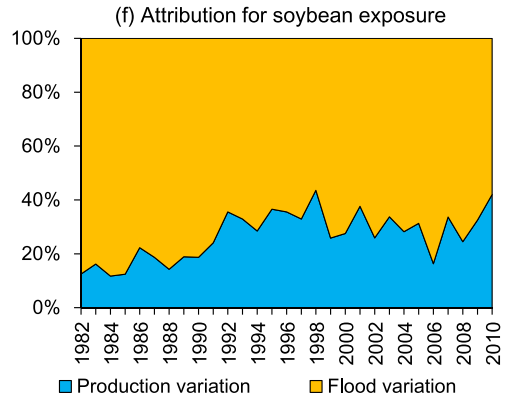
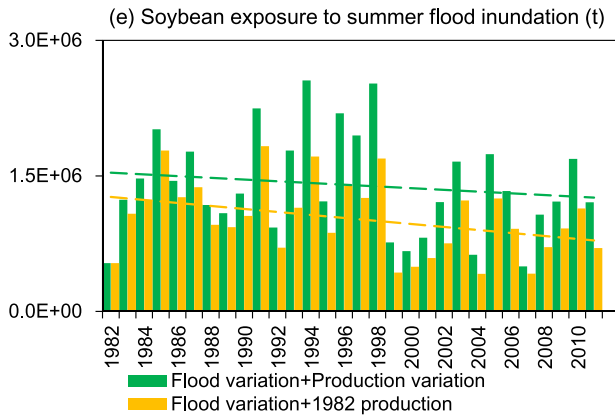
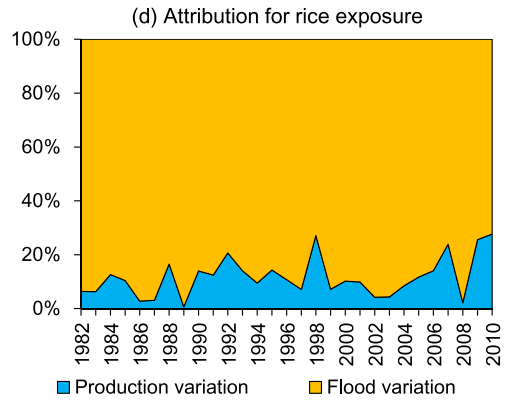
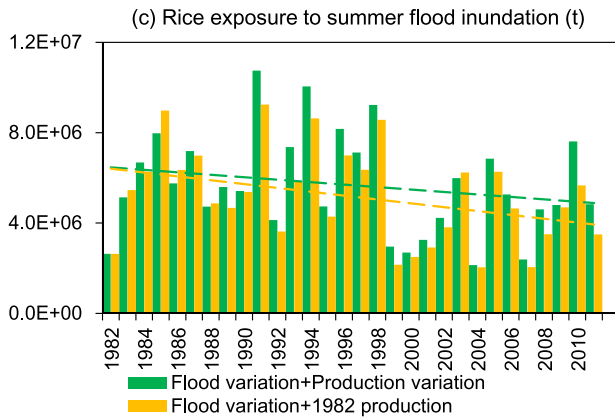
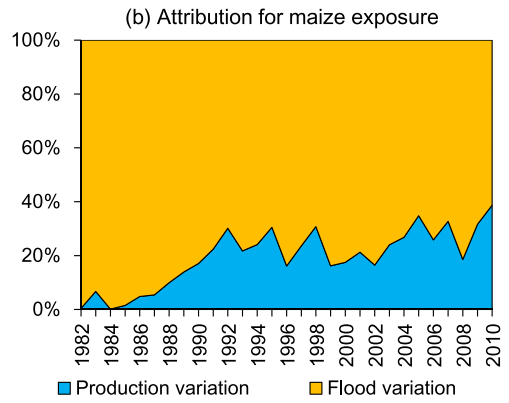
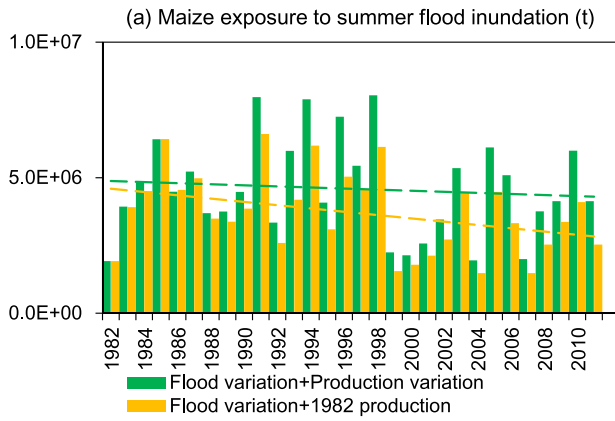


Fig. 4. (a) Potential flood area of summer maximum floods. (b) Potential flood area of spring floods. (c) Summer maximum precipitation. (d) Spring maximum runoff and snow runoff ratio of the spring maximum runoff. (e) Spring maximum precipitation. ‘Sig’ = Significant.



**Fig. 5.** Potential crop production exposures to summer and spring floods and attribution of the potential exposures to crop production and flood variations.

to summer maximum floods is even decreasing when ignoring enlargement of economic volume, and spring flood influenced GDP is minor compared to summer flood influence. Therefore, sustainability measures should be taken to develop the economy and reduce the potential flood influence on development at the same time, and flood management should focus on summer floods.

3.7. Discussion

The total number of large and moderate reservoirs was 217 in 1988 and 343 in 2008, according to the water resources report of the Songliao River Water Resources Commission, Ministry of Water Resources, the People’s Republic of China ([www.mwr.gov.cn/english/](http://www.mwr.gov.cn/english/)). Operation rules vary with dams, and detailed information on the dam operation rules for flood control is currently not available. In addition, dike heights vary along river channels, and spatially distributed dike height information is also currently not available. It is challenging to simulate the influence of such many dams and varying dike heights without detailed information. Considering the importance of potential flood risk and the limited dam and dike information, we studied the potential flood risk in this study.

Fig. S3 shows the probability of flooding under various flood depth thresholds. The probability is calculated as the ratio of the number of days with flood depths greater than the thresholds to the total number of days. The various flood depth thresholds represent potential flood dike heights. The probability generally decreases with increasing thresholds. When the flood depth threshold is 1.5 m, a large area in the Songhua River still has potential flooding risk (Fig. S3b). Because there are 1.5 m or higher flood dikes along the lower reaches of the Liao River, the satellite observed water area (Fig. S1d) is similar to the results of the 1.5 m flood depth threshold in the Liao River (Fig. S3d).

The global surface water occurrence dataset provides multiyear mean values based on satellite data from 1984 to 2018. Our

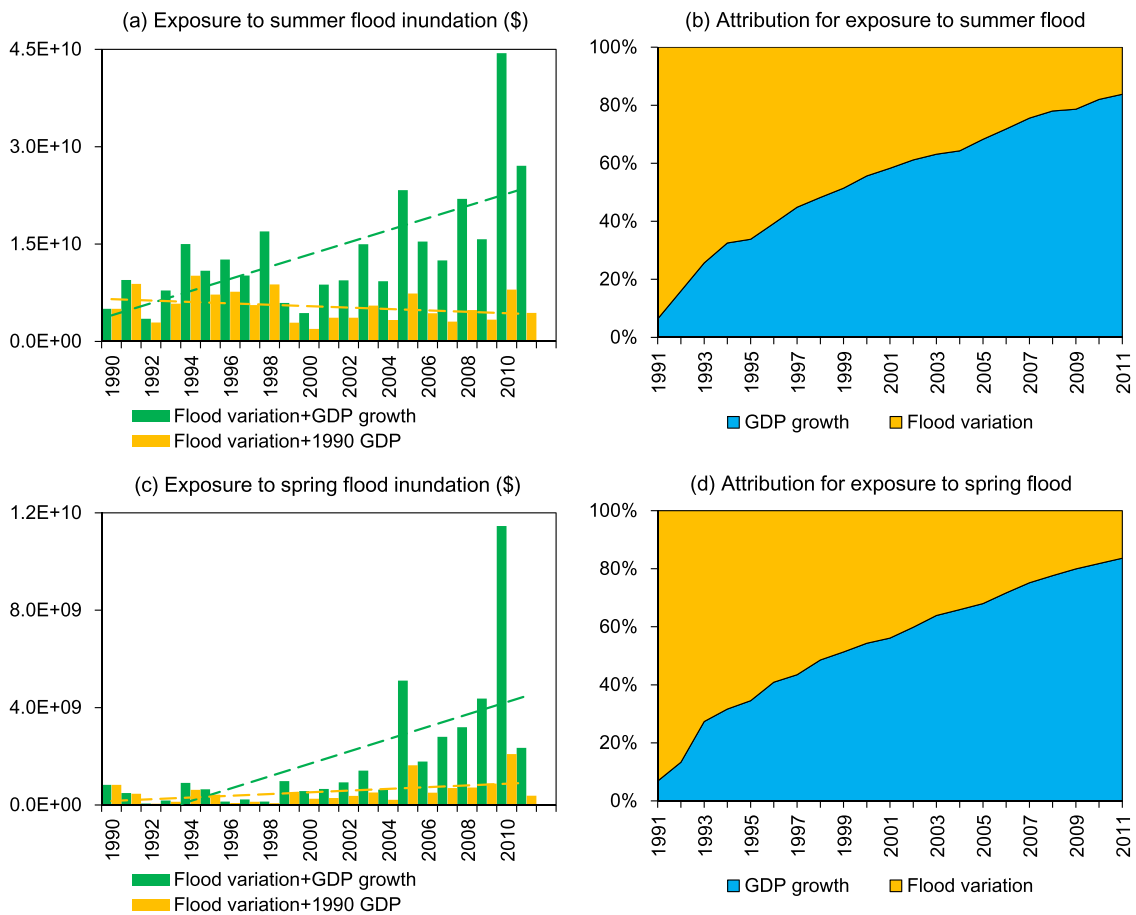


**Fig. 6.** Potential economic exposures to summer and spring floods and attribution of the potential exposures to enlargement of economic volume and flood variations. GDP units = 2011 international US dollar.

simulation is from 1982 to 2011. The differences in the time periods may contribute to the disparity in Fig. S1. However, there is no satellite data product exactly corresponding to the period we investigated. In addition, the comparison is on a multiyear mean scale ( $\geq 30$  years), and the influence of time differences should be minor.

#### 4. Conclusions

As an important area for industry and agriculture, Northeast China suffers from both the spring floods and summer floods. In this region, investigations are lacking in terms of the spatial distribution of snow melt contributions to the spring maximum runoff/discharge, and no studies have compared spring and summer potential flood risks. This study presents important progress in snow melt spring potential flood risk assessment and its comparison with summer potential flood risk in Northeast China. The following conclusions are presented based on this study.

First, snow melt contributes approximately three-fourths of the spring maximum floods. The summer potential flood risk decreased from 1982 to 2011, and the spring potential flood risk increased, but the proportion resulting from snow melt decreased.

Second, potentially exposed food production of maize, rice and soybean to summer floods accounts for approximately 2.8% of the total production, and potentially exposed wheat production to spring floods accounts for 0.3% of the total. Changes in potential crop production exposures to summer and spring floods are dominated by variations in floods.

Third, GDP growth exacerbates the increasing trends of potential economic exposure to both summer and spring floods, and the potential exposure to summer floods is even decreasing when ignoring the enlargement of economic volume. The potential economic exposure to summer floods accounts for 3.9% of the total Northeast China GDP, and it is 0.4% for spring floods.

#### CRedit authorship contribution statement

**Wei Qi:** Conceptualization, Methodology, Writing – original draft. **Lian Feng:** Writing – review & editing. **Hong Yang:** Writing – review & editing. **Junguo Liu:** Writing – review & editing.

#### Declaration of Competing Interest

The authors declare that they have no known competing financial interests or personal relationships that could have appeared to influence the work reported in this paper.

#### Acknowledgements

This study was supported by the Young Scientists Fund of the National Natural Science Foundation of China (51809136), National Natural Science Foundation of China (41971304), the Strategic Priority Research Program of the Chinese Academy of Sciences (XDA20060402), Shenzhen Science and Technology Innovation Committee (JCYJ20190809155205559), Stable Support Plan Program of Shenzhen Natural Science Fund (20200925155151006), Shenzhen Science and Technology Program (KCXFZ20201221173007020), and the High-level Special Funding of the Southern University of Science and Technology (G02296302, G02296402). The hydrological gauge data are from hydrology bureaus and can be found by contacting the Songliao River Water Resources Commission, Ministry of Water Resources, the People's Republic of China (<http://www.mwr.gov.cn/english/>).

#### Appendix A. Supporting information

Supplementary data associated with this article can be found in the online version at [doi:10.1016/j.ejrh.2021.100951](https://doi.org/10.1016/j.ejrh.2021.100951).

#### References

- Chen, H., Liang, Q., Liang, Z., Liu, Y., Xie, S., 2019. Remote-sensing disturbance detection index to identify spatio-temporal varying flood impact on crop production. *Agric. For. Meteorol.* 269–270, 180–191.
- Chen, H., Liang, Z., Liu, Y., Jiang, Q., Xie, S., 2018. Effects of drought and flood on crop production in China across 1949–2015: spatial heterogeneity analysis with Bayesian hierarchical modeling. *Nat. Hazards* 92 (1), 525–541.
- Fu, Q., Zhou, Z., Li, T., Liu, D., Hou, R., Cui, S., Yan, P., 2018. Spatiotemporal characteristics of droughts and floods in northeastern China and their impacts on agriculture. *Stoch. Environ. Res. Risk Assess.* 32 (10), 2913–2931.
- Iizumi, T., Sakai, T., 2020. The global dataset of historical yields for major crops 1981–2016. *Sci. Data* 7, 907.
- Kent, C., Pope, E., Thompson, V., Lewis, K., Scaife, A.A., Dunstone, N., 2017. Using climate model simulations to assess the current climate risk to maize production. *Environ. Res. Lett.* 12 (5), 054012.
- Kummu, M., Taka, M., Guillaume, J.H.A., 2018. Gridded global datasets for Gross Domestic Product and Human Development Index over 1990–2015. *Sci. Data* 5 (1), 180004.
- Lehner, B., Liermann, C.R., Revenga, C., Vörösmarty, C., Fekete, B., Crouzet, P., Doll, P., Endejan, M., Frenken, K., Magome, J., Nilsson, C., Robertson, J.C., Rödel, R., Sindorf, N., Wisser, D., 2011. High-resolution mapping of the world's reservoirs and dams for sustainable river-flow management. *Front. Ecol. Environ.* 9 (9), 494–502.
- Liu, X., et al., 2018. Multimodel assessments of human and climate impacts on mean annual streamflow in China. *Hydrol. Earth Syst. Sci. Discuss.* 1–27.
- Messager, M.L., Lehner, B., Grill, G., Nedeva, I., Schmitt, O., 2016. Estimating the volume and age of water stored in global lakes using a geo-statistical approach. *Nat. Commun.* 7, 13603.
- Qi, W., Feng, L., Liu, J., Yang, H., 2020. Snow as an important natural reservoir for runoff and soil moisture in Northeast China. *J. Geophys. Res. Atmos.* 125 (22), 2201.

- Qi, W., Liu, J., Chen, D., 2018. Evaluations and improvements of GLDAS2.0 and GLDAS2.1 forcing data's applicability for basin scale hydrological simulations in the Tibetan Plateau. *J. Geophys. Res. Atmos.* 123 (23), 13128–13148.
- Qi, W., Liu, J., Leung, F., 2019. A framework to quantify impacts of elevated CO<sub>2</sub> concentration, global warming and leaf area changes on seasonal variations of water resources on a river basin scale. *J. Hydrol.* 570, 508–522.
- Qi, W., Zhang, C., Fu, G., Sweetapple, C., Zhou, H., 2016. Evaluation of global fine-resolution precipitation products and their uncertainty quantification in ensemble discharge simulations. *Hydrol. Earth Syst. Sci.* 20 (2), 903–920.
- Qi, W., Zhang, C., Fu, G., Zhou, H., 2015. Global Land Data Assimilation System data assessment using a distributed biosphere hydrological model. *J. Hydrol.* 528, 652–667.
- Shrestha, M., Wang, L., Koike, T., Xue, Y., Hirabayashi, Y., 2010. Improving the snow physics of WEB-DHM and its point evaluation at the SnowMIP sites. *Hydrol. Earth Syst. Sci.* 14 (12), 2577–2594.
- Tian, L., Li, H., Li, F., Li, X., Du, X., Ye, X., 2018. Identification of key influence factors and an empirical formula for spring snowmelt-runoff: a case study in mid-temperate zone of northeast China. *Sci. Rep.* 8 (1), 16950.
- Wang, L., Koike, T., Yang, K., Jackson, T.J., Bindlish, R., Yang, D., 2009b. Development of a distributed biosphere hydrological model and its evaluation with the Southern Great Plains Experiments (SGP97 and SGP99). *J. Geophys. Res. Atmos.* 114 (D8), D08107.
- Wang, L., Koike, T., Yang, D.W., Yang, K., 2009a. Improving the hydrology of the simple biosphere model 2 and its evaluation within the framework of a distributed hydrological model. *Hydrol. Sci. J.* 54 (6), 989–1006.
- Wang, L., Koike, T., Yang, K., Yeh, P.J.-F., 2009c. Assessment of a distributed biosphere hydrological model against streamflow and MODIS land surface temperature in the upper Tone River Basin. *J. Hydrol.* 377 (1–2), 21–34.
- Wang, L., Zhou, J., Qi, J., Sun, L., Yang, K., Tian, L., Lin, Y., Liu, W., Shrestha, M., Xue, Y., Koike, T., Ma, Y., Li, X., Chen, Y., Chen, D., Piao, S., Lu, H., 2017. Development of a land surface model with coupled snow and frozen soil physics. *Water Resour. Res.* 53 (6), 5085–5103.
- Xin, F., Xiao, X., Dong, J., Zhang, G., Zhang, Y., Wu, X., Li, X., Zou, Z., Ma, J., Du, G., Doughty, R.B., Zhao, B., Li, B., 2020. Large increases of paddy rice area, gross primary production, and grain production in Northeast China during 2000–2017. *Sci. Total Environ.* 711, 135183.
- Yamazaki, D., Almeida, G.A.M., Bates, P.D., 2013. Improving computational efficiency in global river models by implementing the local inertial flow equation and a vector-based river network map. *Water Resour. Res.* 49 (11), 7221–7235.
- Yamazaki, D., Kanae, S., Kim, H., Oki, T., 2011. A physically based description of floodplain inundation dynamics in a global river routing model. *Water Resour. Res.* 47 (4).
- Yamazaki, D., Lee, H., Alsdorf, D.E., Dutra, E., Kim, H., Kanae, S., Oki, T., 2012. Analysis of the water level dynamics simulated by a global river model: a case study in the Amazon River. *Water Resour. Res.* 48 (9), 2012WR011869.
- Yang, D., 1998. Distributed Hydrological Model Using Hillslope Discretization Based on Catchment Area Function: Development and Applications (PHD). University of Tokyo, Tokyo.
- Yang, X., Lin, E., Ma, S., Ju, H., Guo, L., Xiong, W., Li, Y., Xu, Y., 2007. Adaptation of agriculture to warming in Northeast China. *Clim. Change* 84, 45–58.
- Yang, W., Yang, H., Yang, D., 2020. Classifying floods by quantifying driver contributions in the Eastern Monsoon Region of China. *J. Hydrol.* 585, 124767.
- Zhang, Q., Gu, X., Singh, V.P., Kong, D., Chen, X., 2015. Spatiotemporal behavior of floods and droughts and their impacts on agriculture in China. *Glob. Planet. Change* 131, 63–72.
- Zhang, Q., Gu, X., Singh, V.P., Liu, L., Kong, D., 2016. Flood-induced agricultural loss across China and impacts from climate indices. *Glob. Planet. Change* 139, 31–43.
- Zhu, J., Song, C., Wang, J., Ke, L., 2020. China's inland water dynamics: the significance of water body types. *Proc. Nat. Acad. Sci.* 117, 13876–13878.